

Sensitivity experiments with an adaptation model of circulation of western tropical Indian Ocean

N. Bahulayan¹, C. Shaji², A. D. Rao² & S. K. Dube²

¹ Physical Oceanography Division, National Institute of Oceanography, Dona Paula, Goa 403004, India.

² Centre for Atmospheric Sciences, Indian Institute of Technology, Hauz Khas, New Delhi 110016, India.

Received 23 April 1996; revised 16 July 1996

One 18-level adaptation model of circulation with a flat bottom at 900 m depth has been used to study the sensitivity of the solution to different magnitudes of eddy viscosity and diffusivity coefficients. Three numerical experiments conducted showed that the magnitude and directions of current have not changed substantially, although the horizontal exchange coefficients have been increased by one order and vertical eddy diffusivity coefficients have been increased by 10 times. Computed circulation at 10 m depth is controlled by both wind stress and sea surface topography. Circulation at 50 m depth is mainly controlled by thermohaline forcing and sea surface topography. The current speed in the western tropical Indian Ocean is of the order of 75 to 100 cm sec⁻¹.

Sensitivity tests are one of the essential components of the development of mathematical models of geophysical fluid system. Generally, in large scale ocean circulation models, the eddy coefficients, through which the fluxes of heat, salt and momentum are represented, are parameterised either in terms of known measurable variables or with constant values. The best way to obtain reasonable values of these coefficients is to make microstructure measurements of physical oceanographic variables such as currents, temperature and salinity at different environmental conditions and then compute the values of these coefficients through appropriate empirical and semi-empirical formulas. Such empirically determined values could be used in circulation models to obtain a reasonable picture of circulation of a particular area. Until now, there has not been any such measurement for the computation of eddy coefficients in the Indian Ocean area.

In diagnostic and semi-diagnostic models of ocean circulation, which are intended to obtain steady state mean circulation, it is not essential to parameterise these eddy coefficients. Appropriate constant values of eddy coefficients, which can be obtained through numerical experiments, can be used in such models of ocean circulation. However, prognostic ocean circulation models capable of predicting ocean climate on decadal time scale should have realistic parameterisation of these coefficients¹. In the present paper, three numerical

experiments have been performed to investigate the sensitivity of a multilevel adaptation model of circulation to different values of coefficients. The main scientific rationales for conducting such numerical experiments are to suggest suitable values, of frictional parameters and their range for the computation of ocean currents in the model area. Other objectives of this model study are to study the steady state climatological circulation and also to understand the role of wind and internal density field on generation of 3-dimensional flow field in the western tropical Indian Ocean during winter season.

Materials and Methods

Numerical model

The present adaptation model utilizes the basic hydrothermodynamical equations governing the large scale 3-dimensional flows in spherical co-ordinate system given by Gill². A brief description of the characteristics of the model are presented here. Model (Fig. 1) has a maximum depth of 900 m, resolution of 1° in the zonal and meridional directions and 18 levels in the vertical which are standard oceanographic depths. The present model differs from classical primitive equation models in three aspects: first, the model equations are written in terms of co-latitude of the place, instead of latitude and hence sine and cosine functions of the model equations are modified; second, the spherical co-ordinate system used is different with co-latitude taken positive towards south and vertical axis taken

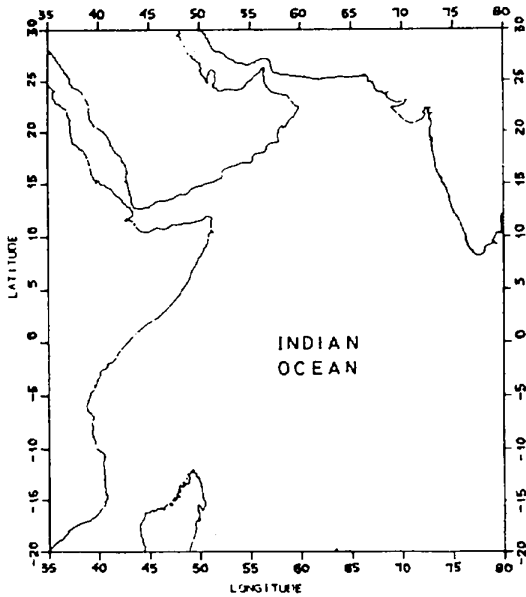


Fig. 1—Location of the model area.

positive in the downward direction; third, the entire numerical solution is completed in two stages. In the first stage, the flow field is generated diagnostically by solving the diagnostic model equations of momentum, hydrostatic, continuity and sea surface topography only. In the second stage, the above diagnostic model equations together with equations of heat and salt are again solved using the flow field obtained from first stage as initial conditions for velocity fields. Such a numerical procedure will save considerable computer time. Considering the above mentioned modifications and approximations of Boussinesq, hydrostatic and incompressibility, the final model equations are written as follows:

$$\frac{\partial u}{\partial t} + Au + lv + \cot \theta \frac{uv}{R} = -\frac{1}{\rho_0 R \sin \theta} \frac{\partial p}{\partial \lambda} + F^\lambda \quad \dots (1)$$

$$\frac{\partial v}{\partial t} + Av - lu + \cot \theta \frac{u^2}{R} = -\frac{1}{\rho_0 R} \frac{\partial p}{\partial \theta} + F^\theta \quad \dots (2)$$

$$\frac{\partial p}{\partial z} = g\rho \quad \dots (3)$$

$$\frac{1}{R \sin \theta} \left[\frac{\partial u}{\partial \lambda} + \frac{\partial (v \sin \theta)}{\partial \theta} \right] + \frac{\partial w}{\partial z} = 0 \quad \dots (4)$$

$$\rho = \rho(T, S) \quad \dots (5)$$

$$\frac{\partial T}{\partial t} + \Delta T = \frac{\partial [v_T \frac{\partial T}{\partial z}]}{\partial z} + \mu_T \Delta T \quad \dots (6)$$

(6)

$$\frac{\partial S}{\partial t} + \Delta S = \frac{\partial [v_T \frac{\partial S}{\partial z}]}{\partial z} + \mu_T \Delta S \quad \dots (7)$$

where

θ - co-latitude = $90 - \phi$, ϕ is the latitude.

u, v, w - the velocity components along the east(λ), south(θ) and downward(z) directions respectively.

p - hydrostatic pressure.

ρ - density of seawater.

ρ_0 - constant density.

R - radius of the Earth.

l - $2\Omega \cos \theta$.

Ω - angular velocity of Earth's rotation.

Au, Av - advective acceleration terms.

F^λ, F^θ - friction terms in the momentum equations.

μ, ν - horizontal and vertical turbulent mixing coefficients respectively.

μ_T, ν_T - horizontal and vertical turbulent diffusion coefficients of heat and salt.

T - temperature.

S - salinity.

$$Af = (Au, Av) = \frac{1}{R \sin \theta} \left[\frac{\partial (uf)}{\partial \lambda} + v \frac{\partial (f \sin \theta)}{\partial \theta} \right] + \frac{\partial (wf)}{\partial z}$$

$$F^\lambda = \frac{\partial \left(\nu \frac{\partial u}{\partial z} \right)}{\partial z} + \mu \left[\Delta u - \frac{1}{R^2 \sin^2 \theta} \left(u - 2 \frac{\partial (v \cos \theta)}{\partial \lambda} \right) \right]$$

$$F^\theta = \frac{\partial \left(\nu \frac{\partial v}{\partial z} \right)}{\partial z} + \mu \left[\Delta v - \frac{v}{R^2 \sin^2 \theta} + \left(\frac{2 \cos \theta}{R^2 \sin^2 \theta} \right) \frac{\partial u}{\partial \lambda} \right]$$

$$\Delta f = (\Delta u, \Delta v) = \frac{1}{R^2 \sin^2 \theta} \frac{\partial^2 f}{\partial \lambda^2} + \frac{1}{R^2 \sin \theta} \frac{\partial (\sin \theta \frac{\partial f}{\partial \theta})}{\partial \theta}$$

Boundary conditions

At the sea surface ($z=0$), we have

$$\rho_0 \nu \frac{\partial u}{\partial z} = -\tau_\lambda; \rho_0 \nu \frac{\partial v}{\partial z} = -\tau_\theta; w|_{z=0} = Q; T|_{z=0} = T^s; S|_{z=0} = S^s \quad \dots (8)$$

where τ_λ and τ_θ are the components of wind stress in the zonal and meridional directions respectively; u, v

are the components of velocity fields and T^* and S^* are the observed temperature and salinity data at the surface.

At the bottom $z=H(\lambda,\theta)$, non-slip boundary condition for velocity fields was applied .

$$i.e. u = v = w = 0 \quad \dots(9)$$

$$\frac{\partial T}{\partial z} = \frac{\partial S}{\partial z} = 0 \quad \dots(10)$$

At the rigid lateral boundaries, the normal flux boundary conditions of zero velocity is prescribed.

$$i.e. \bar{V}_n = 0 \quad \dots(11)$$

$$\frac{\partial T}{\partial \bar{n}} = \frac{\partial S}{\partial \bar{n}} = 0 \quad \dots(12)$$

where 'n' is the normal to the boundary.

There are two open boundaries in the model area; the first zonal open boundary passes through 20°S latitude between the longitudes 35°E and 80°E longitude and the second meridional open boundary passes along the longitude 80°E (Fig. 1). To conserve volume in the model area, component of velocity/flux perpendicular to the open boundary should be balanced. In case the flux/velocity is not balanced, it should be made equal to zero by applying appropriate corrections to the velocity fields. A quasi-geostrophic model³ was used to compute the velocity components at all the levels. The integrated meridional component of velocity was then computed and made equal to zero at the southern open sea boundary. In addition, the u-component of velocity was also prescribed at all levels along the southern open sea boundary. At the north-south open sea boundary that passes along 80°E, the integrated zonal component of velocity calculated with the help of a quasi-geostrophic model was first made equal to zero and then the v-component of velocity was prescribed at all levels along its boundary. The prescribed velocity components were kept constant throughout the model integration.

The temperature and salinity at the open sea boundary were given as follows:

$$T|_L = T^*; S|_L = S^* \quad \dots(13)$$

where T^* and S^* are the observed temperature and salinity data.

Initial conditions

$$(u, v)_{L_0} = 0; (T, S)_{L_0} = (T^*, S^*) \quad \dots(14)$$

The density of sea water ' ρ ' as given in Eq (5) was calculated by UNESCO formula³. The density of seawater can be written as the sum of the average density ' ρ_0 ' and the density anomaly $\rho'(\lambda,\theta,z)$.

Integrating the hydrostatic Eq (3) in the vertical from free surface to depth, the expression for hydrostatic pressure at depth z can be written as:

$$P_z = \rho_0 g \zeta + g \int_0^z \rho' dz \quad \dots(15)$$

where ' ζ ' is the sea surface topography which is otherwise called sea level. While integrating the hydrostatic equation (3) in the vertical from free surface to depth z , the hydrostatic pressure due to a uniform water column ($\rho_0 g z$) is neglected and hence the density anomaly ρ' would automatically convert itself to actual density ρ . In other wards both ρ' and ρ are one and the same. The pressure gradient terms in the momentum Eqs (1) and (2) were computed using Eq (15). It is found that there are eight unknowns ($u, v, w, \rho, p, \zeta, T$ and S) in seven equations and hence an additional equation for sea surface topography has to be derived to have a closed system of eight model equations in eight unknowns.

Derivation of sea surface topography (sea level)

Sea surface topography is a dynamical variable intimately linked to the flow field in the upper mixed and thermocline layers. While the upper mixed layer circulation is essentially controlled by the resultant of wind stress and sea surface slope, the circulation in the thermocline is mainly controlled by the sea surface topography. The slope of the sea surface affects the slope of the thermocline which in turn, affects the thermocline circulation. Both the surface wind stress and interior flow fields are responsible for generating the sea surface slope. Oceanic motions occurring in the main thermocline and above on spatial scales exceeding the Rossby radius of deformation will penetrate vertically to the surface and generate pressure signals which are reflected in the form of sea surface slope. The magnitude of sea surface slope depends on the time and space scales of motion that are occurring in the ocean's interior.

A detailed discussion on the various methods of derivation of sea surface topography equation is given in the works of Demin & Ibraev⁴. However, a

brief description of the procedure to derive the sea level equation is presented here.

The solution of Eqs (1)-(4) considering the equation for hydrostatic pressure (5) is obtained with the help of a leap-frog numerical scheme. By summing the equation of continuity along all levels taking into account the boundary condition at the surface and bottom for vertical velocity ($w=0$), the two dimensional integral continuity equation is obtained. The two dimensional integral continuity equation is the equation for sea surface topography at the internal grid points. By applying the lateral boundary condition for velocity field in the two-dimensional integral continuity equation, the equation for sea surface topography at the solid boundary points are also obtained. The sea surface topography equation at the internal grid points is written as follows:

$$\frac{1}{R \sin \theta} \left[\delta_{\lambda} \bar{u}^{\theta} + \delta_{\theta} \bar{v}^{\sin \theta} \right] = 0 \quad \dots(16)$$

where δ_{λ} and δ_{θ} are the finite difference operators and \bar{u} and \bar{v} are the vertically integrated velocity components in the zonal and meridional direction respectively. Substituting the values of \bar{u} and \bar{v} in the integral continuity equation, the final expression for sea surface topography is written as follows:

$$\frac{1}{R \sin \theta} \left[\delta_{\lambda} (a \delta_{\lambda} \bar{\zeta}^{\theta} + b \delta_{\theta} \bar{\zeta}^{\lambda}) + \delta_{\theta} (a \delta_{\theta} \bar{\zeta}^{\lambda} - b \delta_{\lambda} \bar{\zeta}^{\theta}) \right] \sin \theta = R_s \quad \dots(17)$$

where

$$a = \frac{\Delta t g H}{1 + \left(\frac{\Delta t^2 l^2}{4} \right)}$$

$$b = a l \frac{\Delta t}{2}$$

$$R_s = \frac{1}{R \sin \theta} \left[\delta_{\lambda} \bar{R}_{\lambda}^{\theta} + \delta_{\theta} \left(\bar{R}_{\theta}^{\lambda} \sin \theta \right) \right]$$

$$R_{\lambda} = R_u - \frac{\left(\frac{\Delta t l}{2} R_v \right)}{\left(1 + \frac{\Delta t^2 l^2}{4} \right)}$$

$$R_{\theta} = R_v + \frac{\left(\frac{\Delta t l}{2} R_u \right)}{\left(1 + \frac{\Delta t^2 l^2}{4} \right)}$$

$$R_u = u^{n+1} + \Delta t \left[\frac{1 v^{n+1}}{2} - \left(\frac{g}{\rho_0 R \sin \theta} \int_0^z \frac{\partial \rho'}{\partial \lambda} dz - A u \cot \theta \frac{u v}{R} \right)^n \right] + (F^{\lambda})^{n+1}$$

$$R_v = v^{n+1} + \Delta t \left[\frac{1 u^{n+1}}{2} - \left(\frac{g}{\rho_0 R} \int_0^z \frac{\partial \rho'}{\partial \theta} dz - A v \cot \theta \frac{u v}{R} \right)^n \right] + (F^{\theta})^{n+1}$$

where Δt is the time step and n is the time step number.

The sea surface topography equation (17) is solved by successive overrelaxation technique.

One of the drawbacks of Levitus⁵ data sets on temperature and salinity is that they are collected randomly in space and time and hence suffers from data noises. These data (temperature and salinity) are not adjusted with wind stress and bottom topography. It is, therefore, necessary to adjust the input of density field with wind stress and bottom topography so that mutually adapted model variables are obtained. Semi-diagnostic (adaptation) method is an effective tool to obtain mutually adapted fields of velocities, temperature, salinity and sea surface topography and these fields can be used as better initial fields for simulation models of circulation. In this method, the model was integrated in two stages: in the first stage, the flow field was generated diagnostically by solving the diagnostic model equations of momentum, hydrostatic, continuity and sea level. The model was integrated for approximately one month by which time quasi-stationarity was achieved. Once a quasi-stationarity solution was obtained when flow fields are fully generated, the second stage of model integration is started. At this stage, the entire set of model equations including turbulent diffusion equations of heat and salt (total of 8 equations) are again integrated for another one month using the flow field obtained from first stage as initial conditions for velocity fields. The total integration time for both stages is approximately two months when full stationarity was achieved. In the second stage of model integration mentioned above, the initial input of density field was allowed to change for a while and hydrodynamically adjusted fields of velocities, temperature, salinity and sea surface topography are obtained.

Results and Discussion

The main forcing parameters of the model are the monthly mean wind stress components at the sea surface and thermohaline forcing (density) at

different levels. There have been many studies on the wind field distribution over the Indian Ocean area⁶⁻¹⁰. Recently wind vector atlas has also been prepared by Gohil and Pandey¹¹ using ERS-1 scatterometer data. This climatology atlas is the first of its kind in India. In the present study, the wind data compiled by Hellerman *et al.*¹² are used. Since the model resolution is 1° in the zonal and meridional directions, the original wind data compiled by Hellerman (2°×2°) have been interpolated to 1° resolution by means of a bilinear interpolation technique for the model area (20°S-30°N, 35°E-80°E). The spatial distribution of mean resultant wind stress for the month of January is presented in Fig.2. During the month of January, northeasterly and easterly winds with magnitudes upto 1 dynes cm⁻² are seen throughout the Arabian Sea north of equator. In the doldrums region, wind field is very weak except off Somali and African coasts. Southeasterly winds with magnitudes greater than 1 dynes cm⁻² are observed in the southern hemisphere between 10°S and 20°S latitude. These southeasterly winds turn towards north and east on approaching the equatorial region between 0° and 10°S latitude.

The present version of the model has 18 levels in the vertical with a maximum depth of 900 m and temperature and salinity data have to be provided at all the 18 levels as initial conditions. We used Levitus⁵ monthly mean data on temperature and

seasonal mean salinity as initial conditions. To compute the monthly mean circulation for January, January mean temperature and winter mean salinity have been used since January mean salinity was not available. In this paper, the results of sensitivity experiments for two depths (10 and 50 m) are presented. It was thought most appropriate to present the σ_t diagrams for the above two depths to explain the steady state circulation for the month of January in response to the constant and local forcings of wind stress and density variation.

The σ_t fields at 10 and 50 m depths are presented in Fig.3a and b respectively. σ_t fields decreases gradually from north to south in both the depths, in addition σ_t lines slopes upwards towards the west coast of India at 10 and 50 m depths. Because of the intrusion of high saline waters from Red Sea and Persian Gulf into the Arabian Sea, the σ_t surfaces slopes downward from north to south favouring a density driven current parallel to the σ_t lines. At 50 m depth, a region of high density was located between 5° and 15°S latitude. The density gradient off the southwest Indian coast is very sharp due to the advection of low saline Bay of Bengal waters towards this region by north equatorial current and insufficient mixing of Bay of Bengal and Arabian Sea waters.

Three numerical experiments were conducted to study the model solution to different friction and diffusivity coefficients. A summary of the various parameter values used in the experiments along with the names of all the coefficients is presented in Table 1. In the first numerical experiment, comparatively low values are used for all the coefficients. The vertical friction coefficients is kept constant at 10 cm² sec⁻¹ in all the three numerical experiments.

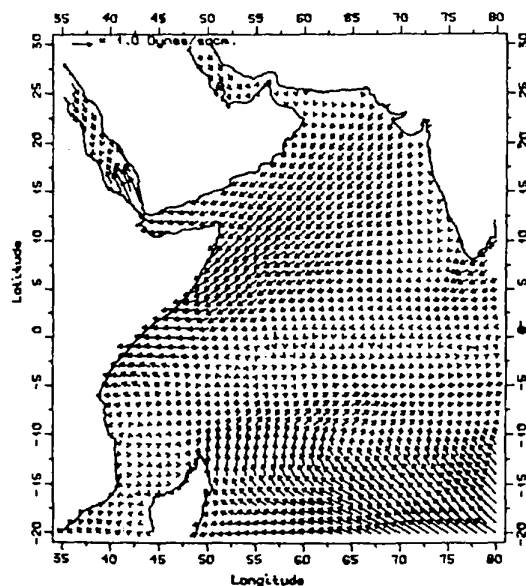


Fig. 2—Observed January mean resultant wind stress.

Table 1—Summary of parameter values used in the sensitivity experiment

Sl. No	Name of the parameters	Notation	Parameter values used		
			Expt. No.1	Expt. No.2	Expt. No.3
1.	Horizontal turbulent mixing coefficient	μ	5×10^7	10^8	5×10^8
2.	Vertical turbulent mixing coefficient	ν	10	10	10
3.	Horizontal turbulent diffusion coefficient	μ_T	5×10^7	10^8	5×10^8
4.	Vertical turbulent diffusion coefficient	ν_T	1	5	10

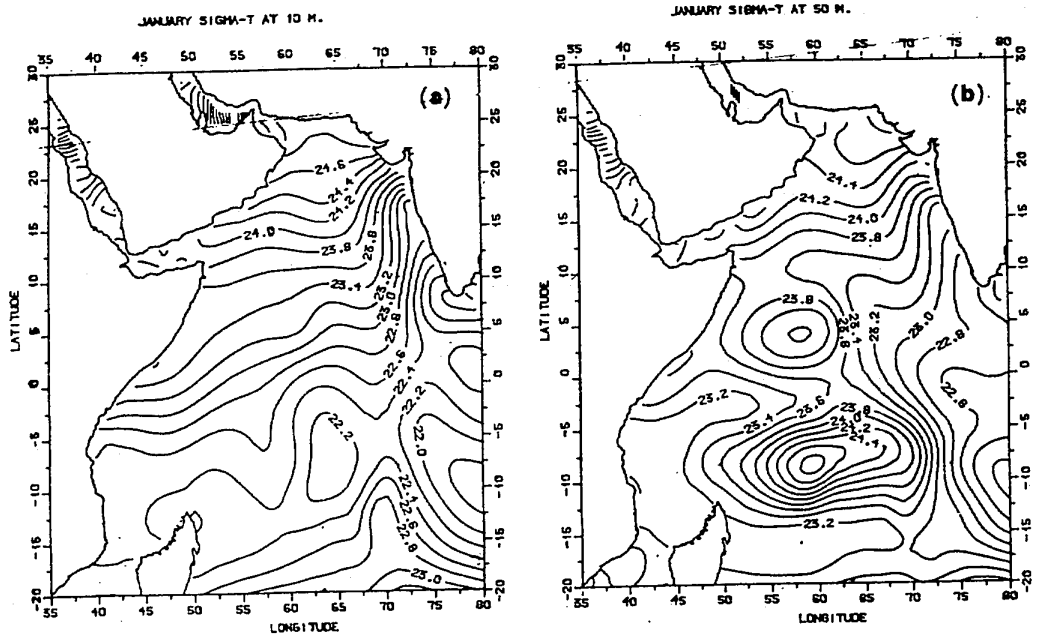


Fig. 3—Spatial distribution of σ_T (a) at 10 m (b) at 50 m depth.

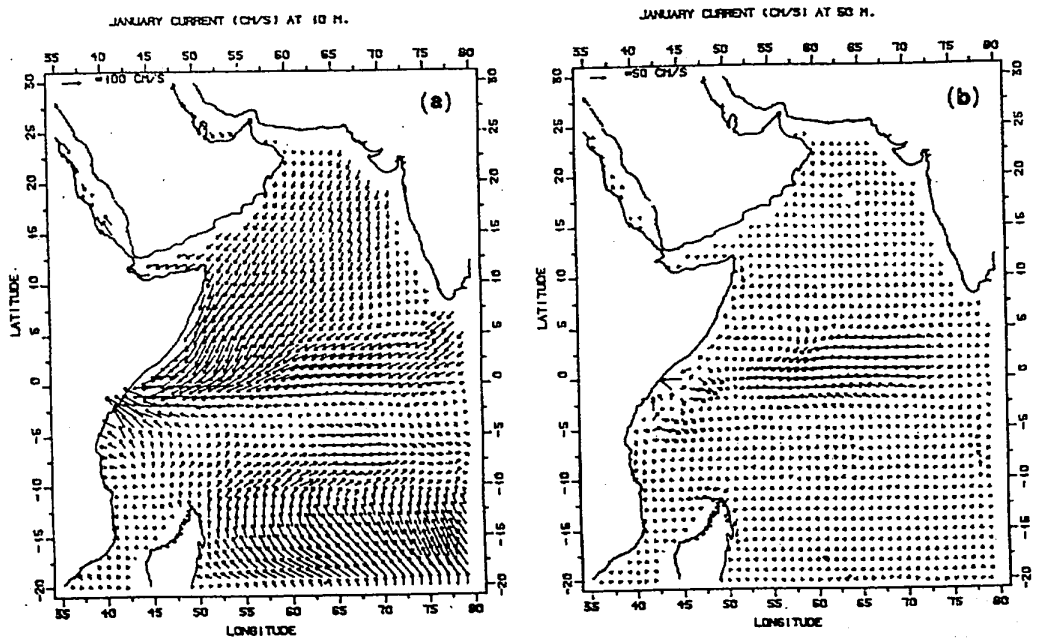


Fig. 4—Computed circulation during the first numerical experiment for the month of January (a) 10 m (b) 50 m depth.

In the first experiment, both the horizontal eddy viscosity and diffusivity coefficients were kept at $5 \times 10^7 \text{ cm}^2 \text{ sec}^{-1}$ (Table 1). The computed currents at 10 and 50 m depths are presented in Fig. 4a and b

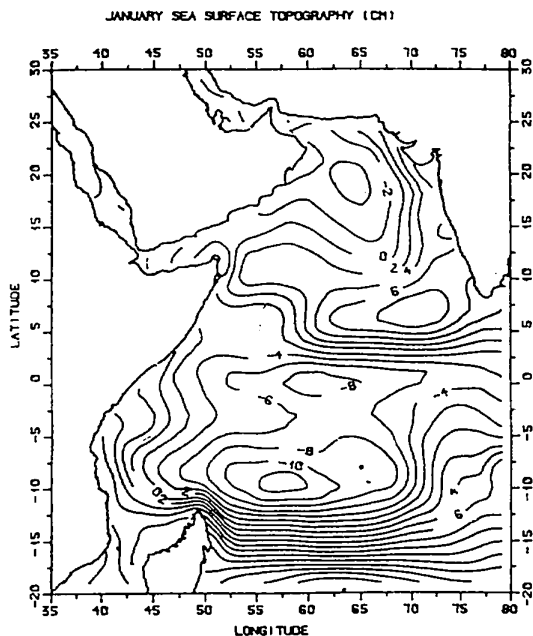


Fig. 5—Computed sea surface topography (cm) for the month of January during the first numerical experiment.

respectively. The sea surface topography calculated on the basis of experiment No.1 is presented in Fig. 5. It is possible to compare the model computed topography with satellite derived values such as ERS-1/2 or TOPEX/POSEIDON data. Analysis of the computed current at 10 m depth indicates that flow fields are generally towards south and southwest in the entire Arabian Sea north of 5°N latitude in response to northerly and northeasterly wind. Another interesting finding is that computed current do not deflect much to the right of the wind direction as expected mainly due to the effect of friction and sea surface topography. The density gradient is from north to south and this, in turn, pushes the water more towards south. In addition, fairly high horizontal friction coefficient used in the model influence the turning of the current towards the right of the wind direction. Between 5°N and equator, the flow field is generally towards west and southwest in response to easterly winds over the regions, showing that wind is the dominant driving force for the generation of North Equatorial Current. The current speed in the western equatorial and Somali region is generally high of the order of 75 to 100 cm sec^{-1} . Between the equator and 10°S latitude, the circulation is mainly driven by wind stress forcing as can be seen from a comparative

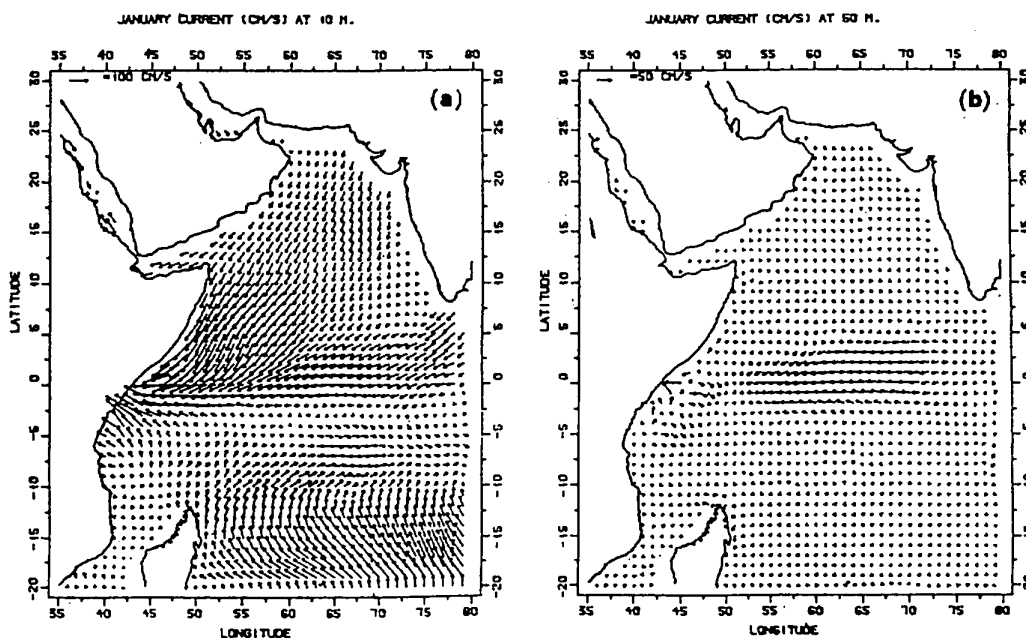


Fig. 6—Computed circulation during the second numerical experiment for the month of January (a) 10 m (b) 50 m depth

study of wind stress and current pattern. A fairly strong Equatorial Counter Current that originates from about 45°E longitude is observed between the equator and 10°S latitude. A broad South Equatorial

Current that flows on a westerly and north westerly direction is located between 10°S and 20°S latitude.

The computed circulation at 50 m depth (Fig. 4b) shows a weak cyclonic circulation in the entire Arabian Sea north of 10°N latitude and the same can be attributed to the combined effects of sea surface topography, density variation and coastal configuration. The northerly circulation along the west coast of India is mainly caused by sea surface topography which slopes upwards towards the coast causing a northward alongshore geotropic flow. In the equatorial regions south of 5°N latitude, wind is still the dominant forcing function that controls the circulation. A weak Equatorial Under Current is observed between 7.5 and 2.5°S latitude.

In the second sensitivity experiment, the horizontal eddy viscosity and diffusivity coefficients have been increased by two-fold and the vertical diffusivity has been increased by five times to study the combined effects of these parameters on the model solution. The computed currents at 10 and 50 m depths are presented in Fig. 6a and b respectively. The sea surface topography for the second experiment is presented in Fig. 7. Comparative study of Figs 6a and 4a show that circulation patterns at this depth were not changed when the coefficients have been changed as mentioned above. The only difference observed was that the magnitude of

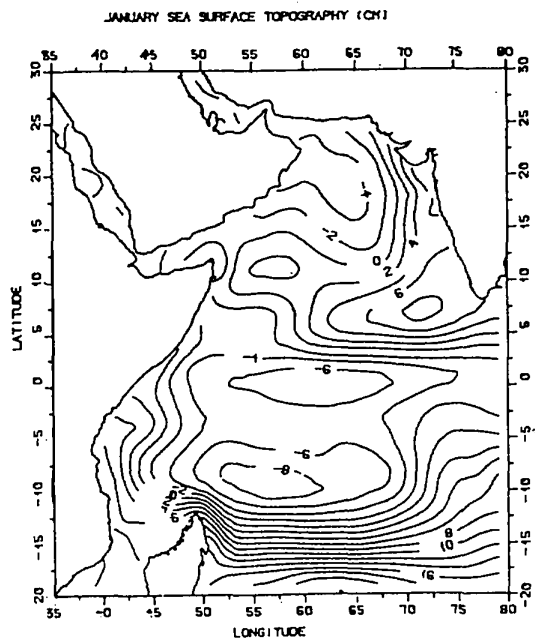


Fig. 7—Computed sea surface topography (cm) for the month of January during the second numerical experiment.

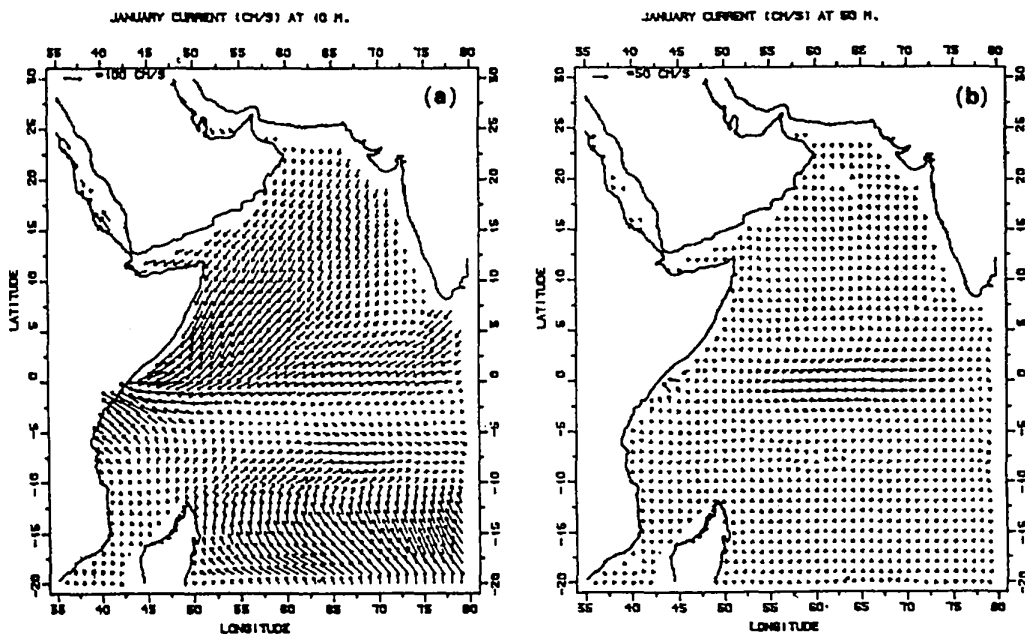


Fig. 8—Computed circulation during the third numerical experiment for the month of January (a) 10 m (b) 50 m depth

current was decreased marginally by 2 to 3 cm sec⁻¹ as compared to first experiment (Fig. 6a). The marginal decrease in the intensity of currents can be attributed to the use of higher values of horizontal eddy viscosity coefficients. At 50 m depth, the magnitude of current was decreased by 5 to 7 cm sec⁻¹ and the direction of current was modified by a

few degrees. However, the general pattern of circulation did not change substantially. Maximum changes in the directions were noticed in the equatorial regions where the currents have become more zonal as compared to first experiment. Effects of horizontal and vertical friction were felt at 50 m depth than at 10 m depth because of strong shear of currents in the equatorial currents.

In the third experiment, the vertical eddy diffusivity coefficient was changed from 5 to 10 cm² sec⁻¹ and the horizontal eddy viscosity and diffusivity coefficients have been changed to 5 × 10⁸ cm² sec⁻¹. The computed currents at 10 and 50 m depths are presented in Fig. 8a and b respectively. The sea surface topography for the third experiment is presented in Fig. 9. The circulation pattern at 10 m depth in terms of both magnitude and direction are almost identical to that of the second experiment. The difference in magnitude of current between the second and third experiment is of the order of 1 cm sec⁻¹ and less only. The intensity of the modulus of current at 10 and 50 m depth along the equator for all the three experiments is presented in Fig. 10a and b. At 10 m depths, the difference in magnitude of currents between different numerical experiments are negligible. However, a difference of 5 to 7 cm sec⁻¹ in intensity was noted at 50 m depth between the first and second experiment because of the two fold increase in the horizontal mixing coefficient.

It has been found from three numerical experiments that the magnitude and directions of

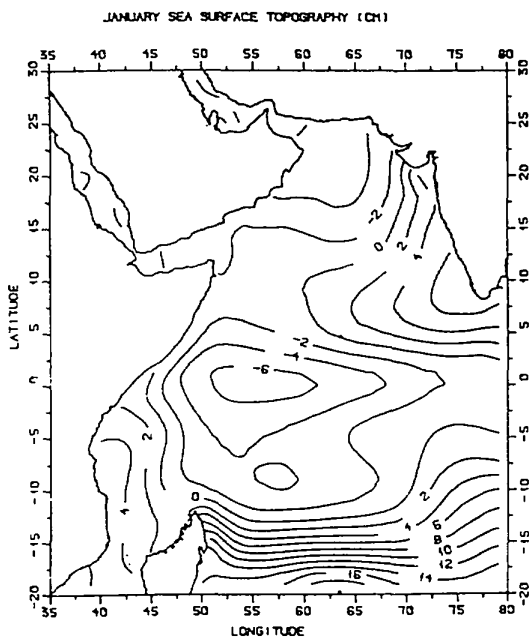


Fig. 9—Computed sea surface topography (cm) for the month of January during the third numerical experiment.

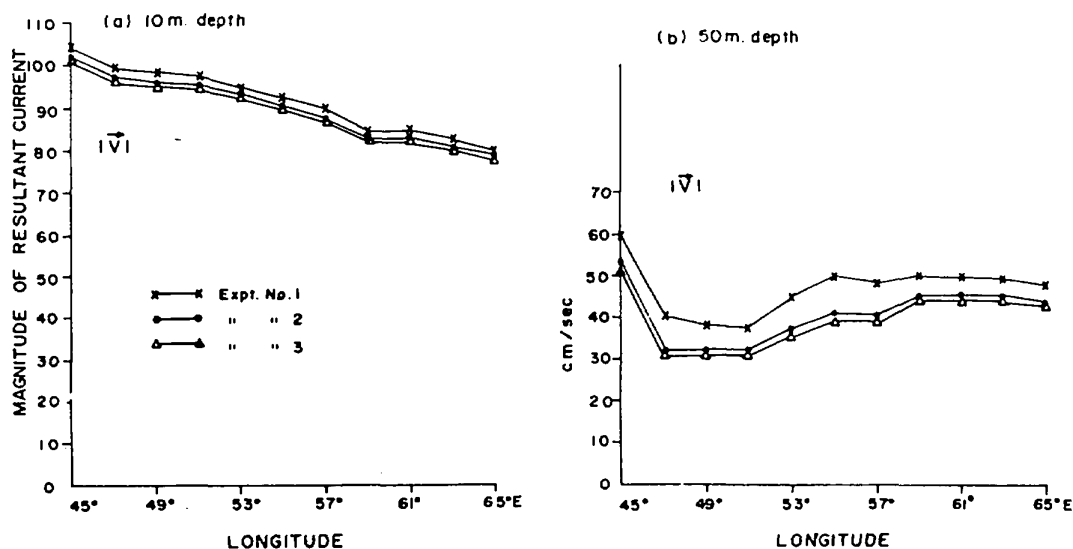


Fig. 10—Intensity of resultant current at (a) 10 m and (b) 50 m depth along the equator for different numerical experiment.

currents have not changed substantially, although the horizontal exchange coefficients have been increased by one order and vertical eddy diffusivity coefficients have been increased by 10 times. The normal range of horizontal eddy viscosity coefficient for the calculation of large scale currents in the Indian ocean is from 5×10^7 to $5 \times 10^8 \text{ cm}^2 \text{ sec}^{-1}$. The computed circulation at 10 m depth is controlled by both wind stress and sea surface topography, although the influence of latter has been found to be very limited. At 50 m depth, thermohaline forcing and sea surface topography considerably influence the circulation. In general, the model has been successful in reproducing the circulation in the Arabian Sea except the surface circulation along the south-west coast of India where remote forcing has a significant influence. The surface circulation along the south-west coast of India is not controlled by local forcings of wind stress and density gradients. The semi-diagnostic model is intended only for computing the large scale climatological mean circulation and also for understanding the role of wind and internal density field on the generation of 3-dimensional flow field.

Acknowledgement

Authors are grateful to the Director, NIO and Head, Data Division, NIO for providing the necessary facilities. One of the authors (C.Shaji)

expresses his gratitude to CSIR for awarding him a Senior Research Fellowship during which this work was carried out. Authors are also grateful to the Department of Science & Technology, New Delhi, for financial assistance.

References

- 1 Woods J D, *Nature*, 314 (1985), 505.
- 2 Gill A E, *Atmosphere-ocean dynamics*, (Academic Press, New York) 1982, pp. 662.
- 3 Marchuk G I & A S Sarkisyan, *Mathematical modelling of ocean circulation*, (Springer-Verlag, Berlin) 1988, pp. 292.
- 4 Demin Yu L & R A Ibraev, *Sov J Numer Anal Math Modelling*, 4 (1989) 211.
- 5 Levitus S, *Climatological atlas of the world ocean*, NOAA Prof. Paper 13, (US Govt. Printing Office, Washington D.C.) 1982, pp. 173.
- 6 Hastenrath S & P J Lamb, *Climatic Atlas of Indian Ocean, Part I: Surface circulation and climate* (Wisconsin Press, Madison) 1979, pp. 109.
- 7 Cadet D L & B C Diel, *Mon Wea Rev*, 112 (1984) 1921.
- 8 Bruce J G, *J Geophys Res*, 83 (1978) 963.
- 9 Wylie D P & Hinton B B, *J Phys Oceanogr*, 12 (1982) 186.
- 10 Luther M E, J J O'Brien & A H Meng, in *coupled ocean-atmosphere models*, edited by J C J Nihoul (Elsevier, New York) 1985, 437.
- 11 Gohil B S & P C Pandey, *An atlas of surface wind vectors in the seas around India during August 1992-July 1993 from ERS-1 Scatterometer* (Special Pub., ISRO-SAC-SP-76-95) 1995, pp. 72.
- 12 Helleman S & M Rosenstein, *J Phys Oceanogr*, 13 (1983) 1093.